Novel Closed Form Solution for Orbit Segment Altitude Extrema Over Spherical and Oblate Central Bodies

Darin C. Koblick
Raytheon Intelligence and Space, El Segundo, CA 90245

ABSTRACT

Interest in satellites, missiles, and hypersonic vehicles travelling through low altitude regions has grown in recent years; especially for harnessing atmospheric drag to station keep or change planes. Mission designers are often asked to determine the vehicle min/max altitudes (altitude extrema) to avoid trajectories which burn up in the atmosphere, hit tall mountain ranges, impact the surface, or traverse environments with high particle radiation levels. A novel closed-form solution to compute the surface altitude extrema for any two-body orbit is proposed and extended to oblate spheroids using Halley's method (a root finding technique with cubic convergence). The runtime performance of this novel method is compared to a golden section search root finding algorithm, `fminbnd`, for thousands of orbit segments (consisting of various eccentricities, inclinations, and segment lengths with both spherical and World Geodetic System 1984 ellipsoid models). Experimental results reveal this novel method accelerates runtime performance between three to five orders of magnitude while maintaining solution accuracy within several centimeters of numerically computed extrema. Improving the runtime performance of flight algorithms that solve trajectory optimization and control problems provides tangible mission advantages as it enables additional fuel and time savings while improving fidelity. These novel methods are easy to implement and simple to port to flight hardware as they require little computational overhead, few lines of code, and a small memory footprint.

1. INTRODUCTION

Many methods to search and compute close encounter distances between satellites and celestial bodies have been developed over the last half century. Previously published research includes: close approaches of comet trajectories to outer planets of our solar system [1], analytic methods to determine close approaches between satellites [2], distances between two Keplerian orbits (including hyperbolic) [3], and Minimum Orbit Intersection Distances (MOID) measuring the minimum distance between two celestial bodies [4]. While astronomers and astrodynamicists may be familiar with MOIDs, the formulation provided in this paper directly computes the surface altitude extrema for an arbitrary orbit segment about a primary body (e.g. two-body system).

A variety of astrodynamic applications require minimum and/or maximum altitude constraints on three-dimensional trajectories between two points on a segment such as asteroid impact deflection, requiring a kinetic impactor to strike the asteroid surface normal to the desired velocity change [5] [6], and celestial object imaging via low altitude flybys [7]. The primary astrodynamic application of interest for this approach involves verifying multiple revolution lambert transfer solutions do not intersect the planet surface [8]. The algorithms introduced in this research were inspired by necessity as the runtime penalty for numerically computing altitude extrema was significant. A computationally efficient process to check continuous orbit segments for intersections with planet surface features, occurring at specific altitudes, is derived and developed in the Theory section. Two application examples are given for low earth and hyperbolic orbits in the examples section. Both examples use the spherical earth model method for surface altitude calculations then compare those results using the oblate spheroid model method to calculate the altitude extrema using WGS-84 [9]. The runtime and extrama values are compared to a purely numerical approach using a golden section search root finding algorithm.`fminbnd`.

2. THEORY

An orbit segment, as depicted in Fig. 1, can be defined by initial and final state vectors in a common geocentric cartesian inertial reference frame such that $\vec{r}_0 = \left[r_{x_0}, r_{y_0}, r_{z_0}\right]$, $\vec{v}_0 = \left[v_{x_0}, v_{y_0}, v_{z_0}\right]$, $\vec{r}_f = \left[r_{x_f}, r_{y_f}, r_{z_f}\right]$, and $\vec{v}_f = \left[v_{x_f}, v_{y_f}, v_{z_f}\right]$

are known. For elliptical orbits, the time of flight between the two points, t_f, indicates whether the transfer angle, θ, is greater than 360° and multiple orbit revolutions have occurred.

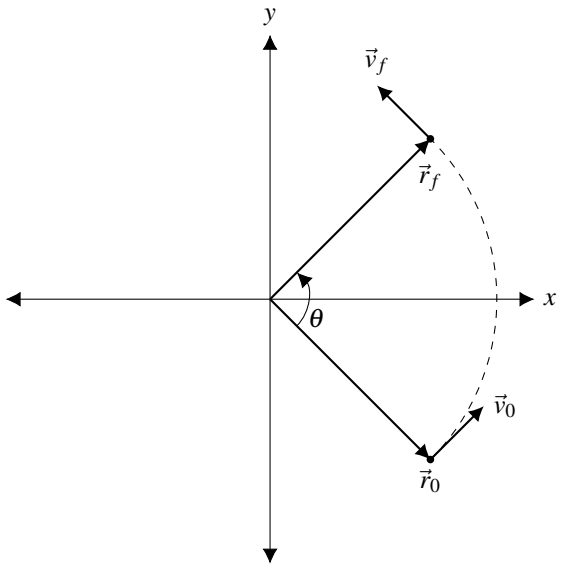

Fig. 1: Orbit Segment Defined by Initial and Final State Vectors

The semi-major axis may be determined from the specific mechanic energy via

$$a = -\frac{\mu}{2\xi} \tag{1}$$

where μ is the standard gravitational parameter of the central body, and the specific mechanical energy, ξ, is a function of the velocity and position magnitudes, r and v, of any point on the orbit such that $\xi = v^2/2 - \mu/r$. The eccentricity vector, for any orbit, can be found from

$$\vec{e} = \frac{\vec{v} \times \vec{h}}{\mu} - \frac{\vec{r}}{r}, \tag{2}$$

where the specific angular momentum, $\vec{h}$, is a function of the cross product of the position and velocity

$$\vec{h} = \vec{r} \times \vec{v}. \tag{3}$$

The true anomaly, ν, for a non-circular orbit, is a function of its eccentricity and position vector such that

$$\nu = \cos^{-1}\left(\frac{\vec{e} \cdot \vec{r}}{er}\right) \tag{4}$$

$$\text{if } \vec{r} \cdot \vec{v} < 0 \text{ then } \nu = 360^\circ - \nu. \tag{5}$$

Note that the true anomaly and argument of perigee, ω, are undefined for circular orbits. If the orbit is circular, the argument of latitude, u is computed from the line of nodes, $\vec{n}$ [10]

$$\vec{n} = \hat{K} \times \vec{h} \tag{6}$$

$$u = \cos^{-1}\left(\frac{\vec{n} \cdot \vec{r}}{nr}\right) \tag{7}$$

$$\text{if } r_z < 0 \text{ then } u = 360^\circ - u. \tag{8}$$

$\hat{K}$ is a unit vector representing the inertial z axis such that $\hat{K} = [0, 0, 1]$. Knowing that the classical relationship between the argument of latitude and true anomaly is

$$u = \nu + \omega, \tag{9}$$

the argument of perigee for circular orbits is zero, $\omega = 0$, and the true anomaly is equal to the argument of latitude, $\nu = u$. The momentum vector aligns with $\hat{K}$ and $\vec{n} \to 0$ when the orbital inclination approaches zero. Therefore, when the orbit is both circular and equatorial, the true longitude, λ_{true} is measured between the position vector and the x-axis such that

$$\lambda_{\text{true}} = \cos^{-1}\left(\frac{r_x}{r}\right) \tag{10}$$

$$\text{if } r_y < 0 \text{ then } \lambda_{\text{true}} = 360^\circ - \lambda_{\text{true}}. \tag{11}$$

The true anomaly is a function of the right ascension of ascending node, Ω, and argument of perigee such that

$$\nu = \lambda_{\text{true}} - \Omega - \omega. \tag{12}$$

Note that for equatorial orbits, the right ascension of ascending node can be set to zero, $\Omega = 0$. While the argument of perigee for an inclined orbits is [11]

$$\omega = \cos^{-1}\left(\frac{\vec{n}\cdot\vec{e}}{ne}\right) \tag{13}$$

$$\text{if } e_z < 0 \text{ then } \omega = 360^\circ - \omega, \tag{14}$$

the argument of perigee for equatorial orbits is equal to the angle between the x and y axis.

$$\omega = \text{atan2}\left(e_y, e_x\right) \tag{15}$$

$$\text{if } \hat{K}\cdot(\vec{r}\times\vec{v}) < 0 \text{ then } \omega = 360^\circ - \omega \tag{16}$$

The number of revolutions contained within a segment is the ratio of the fight time over the orbital period,

$$N_{\text{rev}} = \frac{t_f}{P}, \tag{17}$$

where P is the orbital period written as a function of the semi-major axis

$$P = \begin{cases} 2\pi\sqrt{\frac{a^3}{\mu}} & \text{if } e < 1 \\ \infty & \text{otherwise.} \end{cases} \tag{18}$$

2.1 Determining the Altitude Extrema Over a Sphere

The minimum radius of any orbit occurs at perigee, r_p , corresponding to $\nu = 0^\circ$,

$$r_p = \begin{cases} a(1-e) & \text{if } e \neq 1 \\ \frac{h^2}{2\mu} & \text{otherwise,} \end{cases} \tag{19}$$

and similarly, the maximum radius of an elliptical orbit occurs at apogee, r_a, when the true anomaly is $\nu = 180^\circ$,

$$r_a = \begin{cases} a(1+e) & \text{if } e \neq 1 \\ \infty & \text{otherwise.} \end{cases} \tag{20}$$

A logic check can determine if apogee and perigee are contained within the orbit segment. Since the bounds, ν_0 and ν_f are known, a set of "and" ($\wedge$) "or" ($\vee$) statements determine if a specific true anomaly, ν, is contained between them,

$$(\nu_0 \leq \nu_f \wedge \nu \leq \nu_f) \vee (\nu_0 > \nu_f \wedge \left[0 \leq \nu \leq \nu_f \vee \nu_0 \leq \nu\right]) \implies \nu \in \left[\nu_0, \nu_f\right]. \tag{21}$$

The altitude extrema of any orbit segment over a spherical planet is found by subtracting the planet radius, R, from the radial distance extrema,

$$\text{alt}_{\text{min}} = \begin{cases} r_p - R & \text{if } 0^\circ \in \left[\nu_0, \nu_f\right] \vee N_{\text{rev}} \geq 1 \\ \min\left(r_0, r_f\right) - R & \text{otherwise,} \end{cases} \tag{22}$$

$$\text{alt}_{\text{max}} = \begin{cases} r_a - R & \text{if } \left(180^\circ \in \left[\nu_0, \nu_f\right] \vee N_{\text{rev}} \geq 1\right) \wedge e < 1 \\ \max\left(r_0, r_f\right) - R & \text{otherwise.} \end{cases} \tag{23}$$

Note that a circular orbit is degenerate as there would be no altitude variation over a spherical planet such that $\text{alt}_{\text{min}} = \text{alt}_{\text{max}} = r - R$. A visual flow chart of the algorithm discussed in this section is presented in Fig. 2.

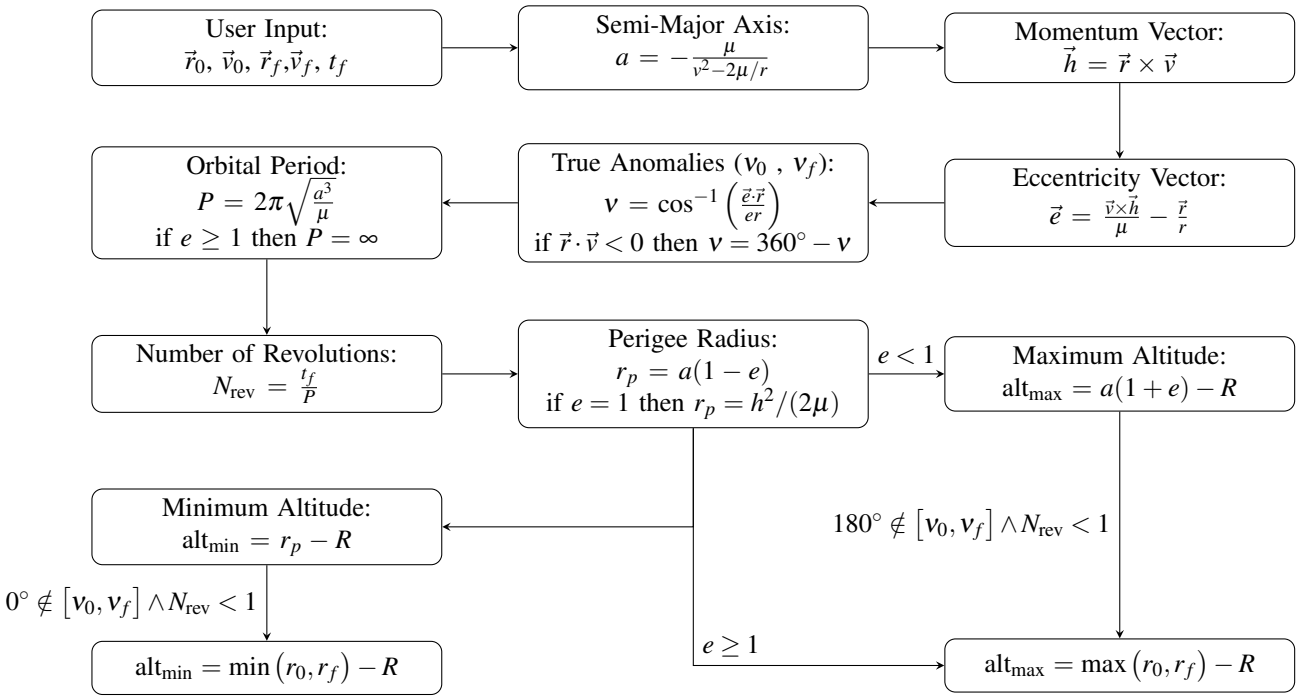

Fig. 2: Flow Chart for Computing the Altitude Extrema Over a Sphere for Non-Circular Orbits

2.2 Determining the Altitude Extrema Over an Oblate Spheroid

The radial distance of a satellite may expressed as a function of its true anomaly,

$$r(\nu) = \frac{h^2}{\mu(1 + e\cos(\nu))}, \tag{24}$$

additionally, the geocentric latitude, ϕ_{gc}, is a function of the argument of latitude (see equations 7 and 9) [12],

$$\phi_{gc}(\nu) = \sin^{-1}[\sin(i)\sin(u)] = \sin^{-1}[\sin(i)\sin(\nu + \omega)], \tag{25}$$

where the inclination, i, is found from the angle between the orbital momentum vector (see equation 3) and the equatorial plane [10],

$$i = \cos^{-1}\left(\frac{h_z}{h}\right). \tag{26}$$

The radius of an oblate oblate spheroid is determined analytically as a function of geocentric latitude [13],

$$R(\phi_{gc}) = \frac{1}{2}[(R_e + R_p) + (R_e - R_p)\cos(2\phi_{gc})], \tag{27}$$

where R_e and R_p are the equatorial and polar radius of the oblate spheroid respectively. For the World Geodetic System (WGS) revision WGS 84, the equatorial radius of Earth is $R_e = 6,378.137$ km while its polar radius is $R_p = 6,356.7523142$ km [9]. The surface altitude is a function of true anomaly and found by subtracting the oblate spheroid surface radius (equation 27) from the radial distance of the satellite (equation 24),

$$\text{alt}(\nu) = \frac{h^2}{\mu(1 + e\cos\nu)} - \frac{1}{2}[(R_e + R_p) + (R_e - R_p)\cos(2\phi_{gc})]. \tag{28}$$

The altitude extrema is obtained by finding the roots to the derivative of equation 28 with respect to true anomaly,

$$\frac{\partial}{\partial \nu}\text{alt}(\nu) = \frac{eh^2 \sin\nu}{\mu(e\cos\nu+1)^2} + (R_e - R_p)\sin^2(i)\sin(2u), \tag{29}$$

further simplifying to

$$f(\nu) = e\sin\nu + c_0 \sin(2u)(e\cos\nu+1)^2 = 0, \tag{30}$$

where

$$c_0 = \frac{\mu(R_e - R_p)\sin^2(i)}{h^2}. \tag{31}$$

Important insight is gained from simplifying to equation 30 and analyzing its roots:

- If the orbit is equatorial or purely retrograde, $i = [0, 180^\circ]$, $c_0 \to 0$, the roots occur near perigee and apogee such that $e\sin\nu = 0$ (e.g. $\nu = [0, 180^\circ]$).
- If the orbit is near circular, $e \to 0$, then the roots correspond to $\sin(2u) = 0$ and may be near $u = [0^\circ, 90^\circ, 180^\circ, 270^\circ]$.
- If the orbit is parabolic, $e \to 1$, then at least one root corresponds to $\nu = 180^\circ$ as equation 30 becomes $\sin\nu + c_0\sin(2u)(\cos\nu+1)^2 = 0$, however, since a parabolic orbit has no apogee, this root must always be discarded.
- If the planet is spherical, $R_e \to R_p$, then $c_0 \to 0$ and the roots to the altitude equation will always correspond to $\sin(\nu)$, or simply $\nu = [0^\circ, 180^\circ]$.

For completeness, solving the simplified root function for all true anomalies provides n approximate solutions for global and local altitude extrema such that

$$\nu_{\text{guess}_k} = \frac{360^\circ}{n}\cdot k,\ k = 0, 1, ..., n-1 \tag{32}$$

$$u_{\text{guess}_k} = \nu_{\text{guess}_k} + \omega \tag{33}$$

Depending on the oblateness parameters (R_e and R_p), the orbit eccentricity and inclination, more than $n = 2$ node points may be required for initial solutions close to all possible roots of equation 30. These node points may be uniformly spaced from 0 to 360° or from solving a similar dynamics problem. Cubic root convergence is achieved using Halley's method [14] as equation 30, a continuous function, is conveniently twice differentiable,

$$\nu_{n+1} = \nu_n - \frac{2f(\nu_n)f'(\nu_n)}{2[f'(\nu_n)]^2 - f(\nu_n)f''(\nu_n)}, \tag{34}$$

where

$$f'(\nu) = 2c_0\left[\cos(2u)(1+e\cos\nu)^2 - \sin(2u)(e+e^2\cos\nu)\sin\nu\right] + e\cos\nu \tag{35}$$

$$f''(\nu) = -2c_0(2e^2\cos(2\nu) + e^2 + 2 + 5e\cos\nu)\sin(2u) - (8c_0(1+e\cos\nu)\cos(2u) + 1)e\sin\nu. \tag{36}$$

Using the initial true anomalies, $\nu_{0_k} = \nu_{\text{guess}_k}$, as a starting value, Halley's method is iterated just several times to converge to a root. There may be more than two roots depending on the eccentricity of the orbit and oblateness of the spheroid. The true anomalies corresponding to the roots of equation 30 are checked to ensure that they're contained within the orbital segment (equation 21). The remaining true anomalies are used in equation 28 to compute the corresponding surface altitude and both the minimum and maximum of the entire set,

$$\text{alt}_{\text{min}} = \min\left\{\text{alt}(\nu_0), \min\left\{\text{alt}(\nu_i)_{i=1}^n\right\}, \text{alt}(\nu_f)\right\},\ \forall\nu_i \in \left[\nu_0, \nu_f\right] \tag{37}$$

$$\text{alt}_{\text{max}} = \max\left\{\text{alt}(\nu_0), \max\left\{\text{alt}(\nu_i)_{i=1}^n\right\}, \text{alt}(\nu_f)\right\},\ \forall\nu_i \in \left[\nu_0, \nu_f\right]. \tag{38}$$

A diagram of the process described above is displayed in Fig. 3. Note that the first several steps are identical to those in section 2.1; Halley's method is included after the computation of the constant coefficient, c_0, to the simplified root function in equation 30.

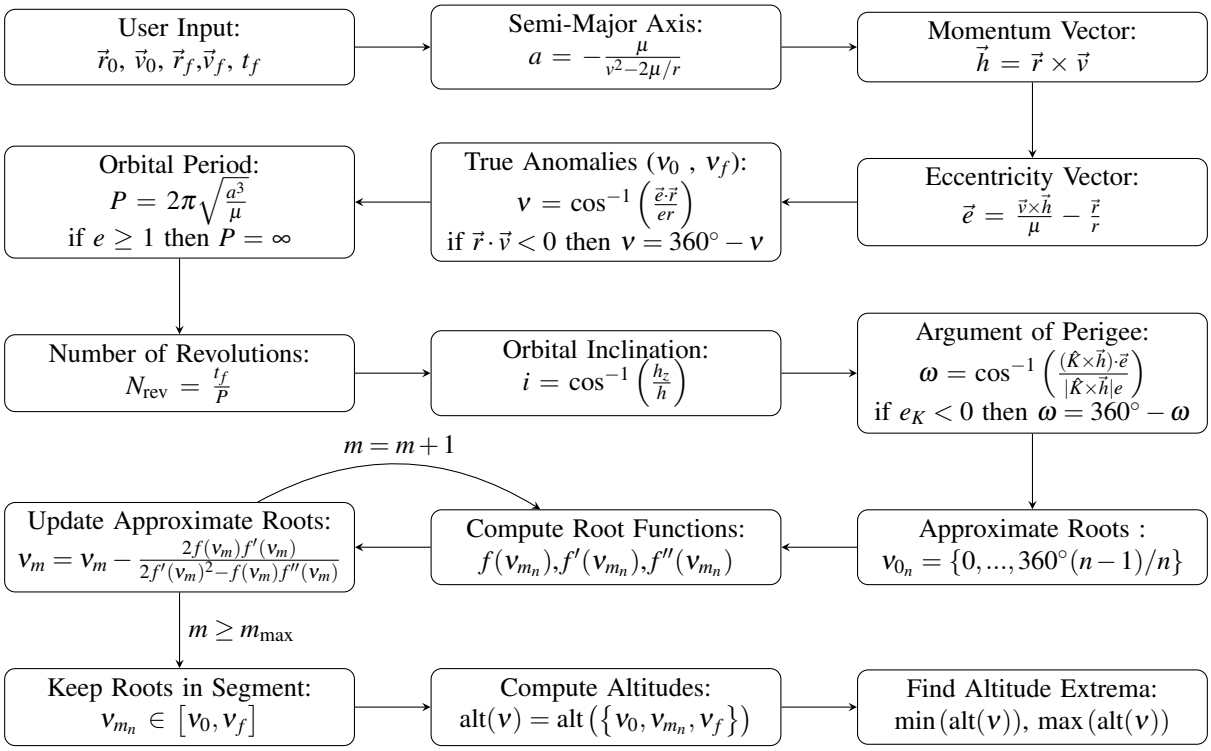

Fig. 3: Flow Chart for Computing the Surface Altitude Extrema over an Oblate Spheroid

3. EXAMPLE APPLICATIONS AND NUMERICAL VERIFICATION

This section determines the altitude extrema for three example applications which include: a slightly eccentric low Earth orbit, a hyperbolic Earth flyby, and thousands of GEO to LEO interceptions. All examples use the WGS-84 parameters for an oblate spheroid and are validated against a numerical golden section search and parabolic interpolation algorithm, `fminbnd` [15]. The first two examples showcase how hand calculatations arrive at the altititude extrema while the last example compares algorithm performance against thousands of trajectories.

3.1 Slightly Eccentric Low Earth Orbit

A low altitude Earth orbit, inclined at 45°, is propagated for a full period, $t_f = 5437.2779$ seconds, such that the initial and final state are equal. The input parameters for both spherical and oblate spheroid models are

$$\vec{r}_0 = \vec{r}_f = \begin{bmatrix} 4722.1472 \\ 3339.0623 \\ 3339.0623 \end{bmatrix} \text{ km}, \quad \vec{v}_0 = \vec{v}_f = \begin{bmatrix} -5.4650 \\ 3.8643 \\ 3.8643 \end{bmatrix} \text{ km/s}.$$

First, the procedure as outlined in section 2.1 is used assuming a spherical Earth radius, R = 6378.137 km, and its standard gravitational parameter , $\mu = 398600.4418$ km/s. Using equation 1, the semi-major axis of the orbit is 6683.137 km, next the momentum vector is computed from equation 3 and used to determine the magnitude of eccentricity in equation 2, $e = 0.00075$. Since the orbit segment consists of a full revolution, the global minimum and maximum surface altitudes correspond to the orbits apogee and perigee. Equations 19 and 20 provide us with the radius of perigee and apogee which were found to be $r_p = 6678.1246$ km and $r_a = 6688.1494$ km respectively. The minimum and maximum altitudes are then determined from equations 22-23, and the corresponding altitude extrema are

$$\text{alt}_{\min} = 299.9876 \text{ km}, \quad \text{alt}_{\max} = 310.0124 \text{ km}.$$

Next, the procedure as outlined in 2.2 is used assuming and oblate Earth with equatorial and polar radii corresponding to $R_e = 6,378.137$ km and $R_p = 6,356.7523142$ km respectively. The orbital inclination is determined using equation 26, $i = 45^\circ$, the argument of perigee is then found from equation 13, $\omega = 45^\circ$.

An grid of six equally spaced true anomalies as defined by equation 32 is used as a starting guess for Halley's method where

$$\nu_n = \begin{bmatrix} 0.000000 & 1.047198 & 2.094395 & 3.141593 & 4.188790 & 5.235988 \end{bmatrix}$$

computing the coefficient to the simplified root function in equation 31, $c_0 = 0.00159989970157076$, and iterating equation 34 four times the true anomalies converge to local extrema altitudes over the orbit.

$$\begin{aligned} \nu_{n+1} &= \begin{bmatrix} 6.072325 & 0.986244 & 2.154945 & 3.353104 & 3.829213 & 5.595245 \end{bmatrix} \\ \nu_{n+2} &= \begin{bmatrix} 5.734358 & 0.986019 & 2.155165 & 3.690969 & 3.784448 & 5.640035 \end{bmatrix} \\ \nu_{n+3} &= \begin{bmatrix} 5.640655 & 0.986019 & 2.155165 & 3.783845 & 3.784394 & 5.640090 \end{bmatrix} \\ \nu_{n+4} &= \begin{bmatrix} 5.640090 & 0.986019 & 2.155165 & 3.784394 & 3.784394 & 5.640090 \end{bmatrix} \end{aligned}$$

There are four unique roots with corresponding altitudes computed by equation 28 such that

$$\text{alt}(\nu_{n+4}) = \begin{bmatrix} 301.202610 & 312.498232 & 308.188882 & 319.487030 \end{bmatrix} \text{ km.}$$

The minimum and maximum of the unique set is taken such that the extrema over a WGS-84 oblate spheroid are found as

$$\text{alt}_{\text{min}} = 301.202610 \text{ km}, \quad \text{alt}_{\text{max}} = 319.487030 \text{ km}.$$

Notice that if the equatorial and polar radii are equal, $R = R_e = R_p = 6378.137$ km, the coefficient to the simplified root function becomes , $c_0 = 0$, and the roots to the equation 30 occur at $\nu = [0^\circ, 180^\circ]$. The minimum and maximum altitude can be determined from further simplifying equation 28 to the magnitude of the satellite position vector at perigee and apogee and subtracting the spherical radius,

$$\text{alt}_{(\text{min,max})} = \frac{h^2}{\mu(1 \pm e)} - R, \tag{39}$$

where the altitude extrema is identical to those values obtained using the spherical altitude extrema procedure as described in section 2.1. A grid of true anomalies ranging from 0 to 360° was created with a resolution of 0.36°, their corresponding altitudes, determined by equation 28, were used to find the global extrema over the interval. The true anomalies corresponding to the global extrema were used to seed the MATLAB implementation of `fminbnd` and further refine results. The minimum and maximum altitudes using this approach were within 1E-12 km of those values obtained for both sphere and oblate spheroid approaches.

3.2 Hyperbolic Earth Flyby

A hyperbolic trajectory, propagated forward by an hour, $t_f = 3600$ seconds , has initial and final inertial state vectors defined as

$$\vec{r}_0 = \begin{bmatrix} 9517.6000 \\ -65.6900 \\ -11737.0000 \end{bmatrix} \text{ km}, \quad \vec{v}_0 = \begin{bmatrix} -1.3216 \\ 3.9369 \\ 6.4404 \end{bmatrix} \text{ km/s}, \quad \vec{r}_f = \begin{bmatrix} -9902.2411 \\ -1139.7502 \\ 10731.6991 \end{bmatrix} \text{ km}, \quad \vec{v}_f = \begin{bmatrix} -6.0537 \\ -4.4720 \\ 1.9370 \end{bmatrix} \text{ km/s}.$$

Using the procedure outlined in section 2.1 with the same values for Earth's radius and standard gravitaional parameter as shown in the first example application in section 3.1, the semi-major axis is $a = -66782.0204$ km, the eccentricity magnitude is $e = 1.1000$, and the initial and final true anomalies, found from equations 4-5, are $\nu_0 = 266.2504^\circ$ and $\nu_f = 92.2143^\circ$ respectively. The orbit does not repeat as the eccentricity is greater than or equal to unity (e.g. no period exists), therefore the minimum altitude corresponds to perigee, $\text{alt}_{\text{min}} = a(1-e) - R$, as $0^\circ \in [266.2504^\circ, 92.2143^\circ]$ and the maximum altitude is the greater of the two position vector magnitudes, $\text{alt}_{\text{max}} = \max(|\vec{r}_0|, |\vec{r}_f|) - R$, such that

$$\text{alt}_{\text{min}} = 300.0056 \text{ km}, \quad \text{alt}_{\text{max}} = 8732.9911 \text{ km}.$$

Following the next procedure in section 2.2 and the same WGS-84 parameters introduced in the first example application (section 3.1), the orbital inclination and argument of perigee are found, $i = 60.00^\circ$ and $\omega = 30.00^\circ$. The

coefficient to the simplified root function is then computed, $c_0 = 0.0011$, and the same equal grid spacing using six true anomalies is used to start Halley's method which is then iterated four times,

$$\begin{aligned}
\nu_n &= \begin{bmatrix} 0.000000 & 1.047198 & 2.094395 & 3.141593 & 4.188790 & 5.235988 \end{bmatrix} \\
\nu_{n+1} &= \begin{bmatrix} 6.279233 & 0.349819 & 2.785381 & 3.141602 & 3.494139 & 5.922457 \end{bmatrix} \\
\nu_{n+2} &= \begin{bmatrix} 6.279233 & 0.004079 & 3.133390 & 3.141602 & 3.149569 & 6.270603 \end{bmatrix} \\
\nu_{n+3} &= \begin{bmatrix} 6.279233 & 6.279233 & 3.141602 & 3.141602 & 3.141602 & 6.279233 \end{bmatrix} \\
\nu_{n+4} &= \begin{bmatrix} 6.279233 & 6.279233 & 3.141602 & 3.141602 & 3.141602 & 6.279233 \end{bmatrix}.
\end{aligned}$$

There are two unique roots, $\nu = [180.0005^\circ, 359.7735^\circ]$ only one of which is contained within the orbital segment, $359.7735^\circ \in [266.2504^\circ, 92.2143^\circ]$, its corresponding altitude is found from equation 28, the maximum altitude is then simply the largest of the three values such that $\text{alt}_{\max} = \max\left[\text{alt}(\nu_0), \text{alt}(\nu_{n+4}), \text{alt}(\nu_f)\right]$,

$$\text{alt}_{\min} = 303.9878 \text{ km}, \quad \text{alt}_{\max} = 8745.8921 \text{ km}.$$

Using the same true anomaly grid resolution of 0.36°, the orbit altitudes contained within the orbital segment were computed. A global minimum and maximum was found for the segment and `fminbnd` was used to further refine the solutions. The minimum altitudes were within machine precision of those values obtained for both the sphere and oblate spheroid approaches; the maximum altitude was not computed using `fminbnd` as it occurs at an endpoint and `fminbnd` searches the interior of an interval ($x_1 < x < x_2$) never evaluating endpoints.

3.3 Geosynchronous to Low Earth Orbit Interception Trajectories

A Lambert two-body solver was used to generate 4,171 individual interception trajectories, originating from an equatorial geosynchronous orbit (GEO) and intercepting a satellite in a 300 km circular polar low Earth orbit (LEO) as shown in Fig. 4. The wait time in the initial orbit was varied in 15 minute increments from the initial orbit epoch to a full day while the transfer duration was varied between one to eight hours in increments of ten minutes. The initial orbit state vectors for both the target and the interceptor are

$$\vec{r}_{tgt_0} = \begin{bmatrix} 0.0000 \\ 0.0000 \\ -6678.137 \end{bmatrix} \text{ km}, \quad \vec{v}_{tgt_0} = \begin{bmatrix} 5.4629 \\ 5.4629 \\ 0.0000 \end{bmatrix} \text{ km/s}, \quad \vec{r}_{int_0} = \begin{bmatrix} 42378.137 \\ 0.0000 \\ 0.0000 \end{bmatrix} \text{ km}, \quad \vec{v}_{int_0} = \begin{bmatrix} 0.0000 \\ 3.0669 \\ 0.0000 \end{bmatrix} \text{ km/s}.$$

The altitude extrema, obtained using both methods, was compared to an implementation of `fminbnd`. For a perfect sphere the relative errors for both minimum (blue) and maximum (red) altitudes are shown in Fig 5. Using the oblate spheroid approach, the relative extrema are shown in Fig 6. The runtime of our altitude extrema implementation for spherical planets, as described in section 2.1, was 0.0006 seconds while the runtime of `fminbnd` was 68.81 seconds, the speedup ratio between the two is therefore five orders of magnitude! Similarly, for the oblate spheroid method described in section 2.2, the runtime was 0.037 seconds while `fminbnd` took 64.71 seconds, resulting in a speedup ratio of three orders of magnitude!

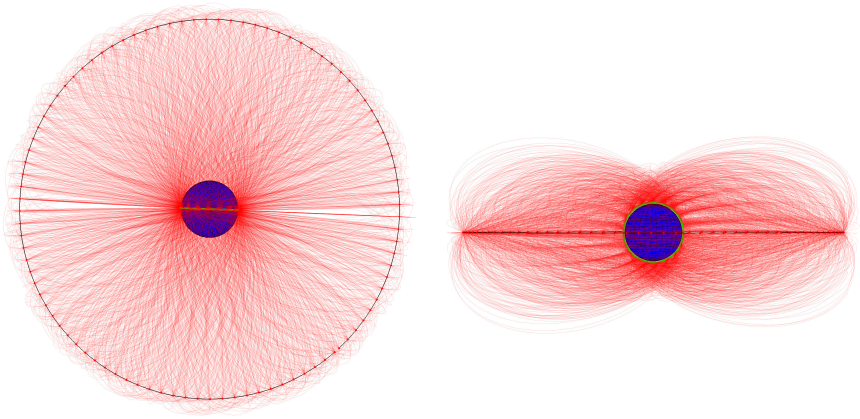

Fig. 4: Polar (left) and Equatorial (right) View of Interception Trajectories from GEO to LEO

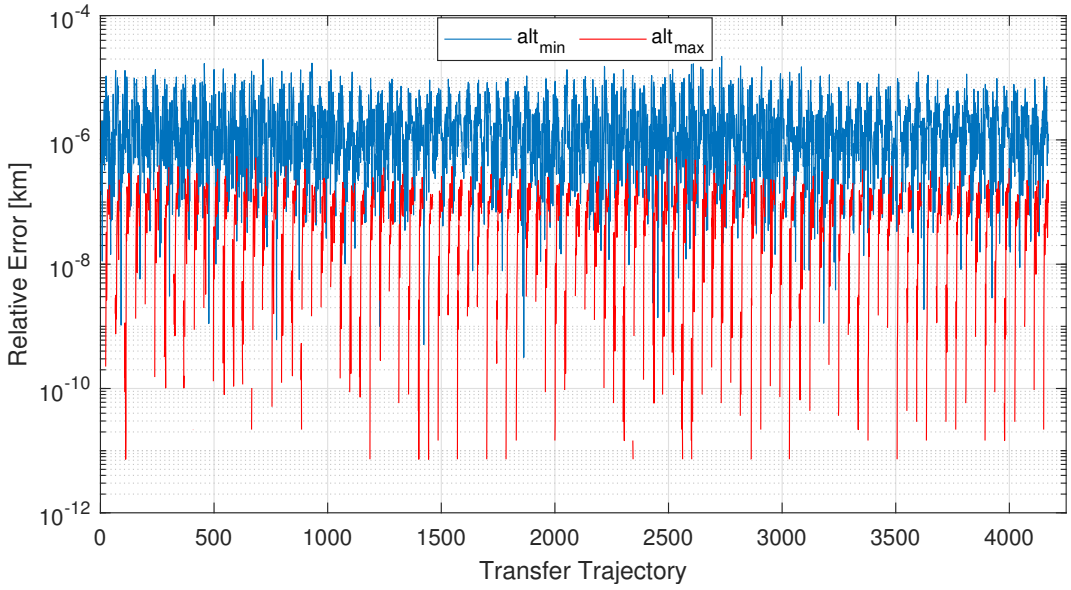

Fig. 5: Relative Error in Altitude Extrema Using a Perfect Sphere

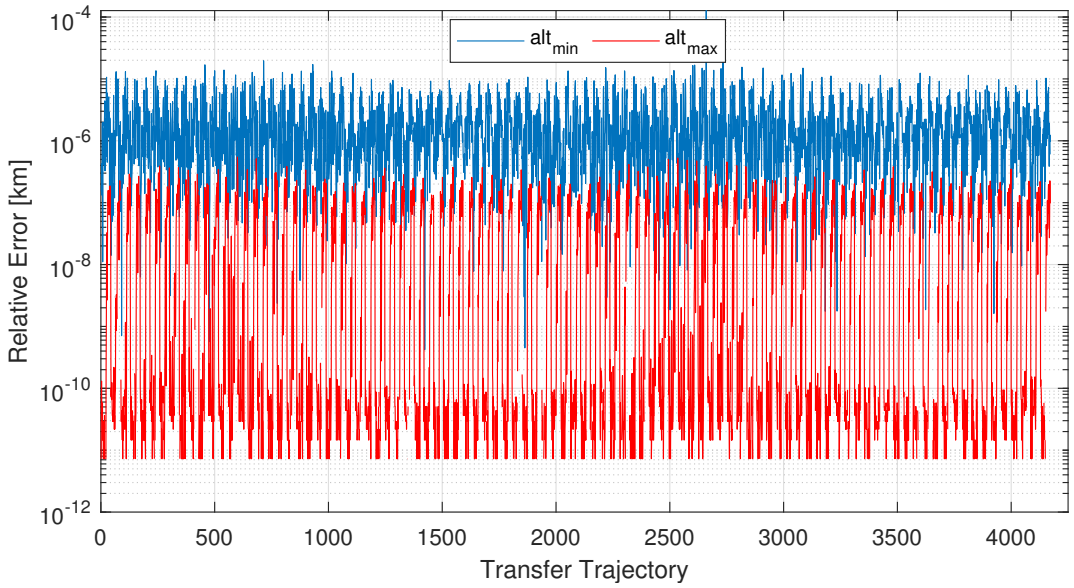

Fig. 6: Relative Error in Altitude Extrema Using a WGS-84 Spheroid

4. CONCLUSIONS AND FUTURE WORK

Two methods for computing the altitude extrema of keplerian orbits have been proposed, derived, and numerically validated. The first method, requiring minimal computational time, determines the exact altitude over spherical central bodies such as planets, moons, and asteroids. If spheroid oblateness effects are desired, the second method approximates the roots of a simple trigonometric function and further refines them using Halley's method. Both methods decrease runtimes between three to five orders of magnitude when compared to a numerical root finding implementation, `fminbnd` with only several centimeters in relative altitude differences. Both methods offer a direct path to flight

hardware as they are easy to implement and require little computational overhead. Future work includes the investigation of the relationship between eccentricity, oblateness, and root placement. Improving the accuracy of the initial true anomaly approximation reduces the number of iterations necessary for high accuracy solutions and improves stability for cases with spheroid oblateness.

5. ACKNOWLEDGMENTS

I'd like to thank J.R Jordan, and Bob Newberry of Raytheon Technologies for their support in funding the preparation of this manuscript. I also want to acknowledge Jeff Heier at Millennium Space Systems for his review and feedback.

6. REFERENCES

[1] G. Sitarski, "Approaches of the parabolic comets to the outer planets," *Acta Astronomica*, vol. 18, p. 171, 1968.
[2] F. R. Hoots, L. L. Crawford, and R. L. Roehrich, "An analytic method to determine future close approaches between satellites," *Celestial mechanics*, vol. 33, no. 2, pp. 143–158, 1984.
[3] R. V. Baluyev and K. V. Kholshevnikov, "Distance between two arbitrary unperturbed orbits," *Celestial Mechanics and Dynamical Astronomy*, vol. 91, no. 3-4, pp. 287–300, 2005.
[4] T. Wisniowski and H. Rickman, "Fast geometric method for calculating accurate minimum orbit intersection distances," *Acta Astronomica*, vol. 63, no. 2, pp. 293–307, 2013.
[5] J. D. Koenig and C. F. Chyba, "Impact deflection of potentially hazardous asteroids using current launch vehicles," *Science & Global Security*, vol. 15, no. 1, pp. 57–83, 2007.
[6] M. Li, Y. Wang, Y. Wang, B. Zhou, and W. Zheng, "enhanced kinetic impactor for deflecting large potentially hazardous asteroids via maneuvering space rocks," *Scientific Reports*, vol. 10, no. 1, pp. 1–9, 2020.
[7] B. Gondet and J.-P. Bibring, "Phobos composition: a reappraisal, based on omega/mex observations," in *EGU General Assembly Conference Abstracts*, p. 11414, 2020.
[8] N. Adurthi and M. Majji, "Uncertain lambert problem: A probabilistic approach," *The Journal of the Astronautical Sciences*, pp. 1–26, 2020.
[9] B. L. Decker, "World geodetic system 1984," tech. rep., Defense Mapping Agency Aerospace Center St Louis Afs Mo, 1986.
[10] G. R. Hintz, *Orbital mechanics and astrodynamics*. Springer, 2015.
[11] Wikipedia contributors, "Argument of periapsis — Wikipedia, the free encyclopedia," 2021. [Online; accessed 16-June-2021].
[12] D. A. Vallado, *Fundamentals of astrodynamics and applications*, vol. 12. Springer Science & Business Media, 2001.
[13] A. Miele, Z. Zhao, and W. Lee, "Optimal trajectories for the aeroassisted flight experiment. part 1: Equations of motion in an earth-fixed system," 1989.
[14] T. Scavo and J. Thoo, "On the geometry of halley's method," *The American mathematical monthly*, vol. 102, no. 5, pp. 417–426, 1995.
[15] G. E. Forsythe, "Computer methods for mathematical computations.," *Prentice-Hall series in automatic computation*, vol. 259, 1977.